



## Iron Alkynyl Helicenes: Redox-Triggered Chiroptical Tuning in the IR and Near-IR Spectral Regions and Suitable for Telecommunications Applications

Chengshuo Shen, Goulc'Hen Loas, Monika Srebro-Hooper, Nicolas Vanthuyne, Loic Toupet, Olivier Cador, Frédéric Paul, Juan T. López navarrete, Francisco J. Ramírez, Belén Nieto-Ortega, et al.

### ► To cite this version:

Chengshuo Shen, Goulc'Hen Loas, Monika Srebro-Hooper, Nicolas Vanthuyne, Loic Toupet, et al.. Iron Alkynyl Helicenes: Redox-Triggered Chiroptical Tuning in the IR and Near-IR Spectral Regions and Suitable for Telecommunications Applications. *Angewandte Chemie International Edition*, 2016, 55 (28), pp.8062-8066. 10.1002/anie.201601633 . hal-01318820

**HAL Id: hal-01318820**

**<https://univ-rennes.hal.science/hal-01318820>**

Submitted on 2 Jun 2016

**HAL** is a multi-disciplinary open access archive for the deposit and dissemination of scientific research documents, whether they are published or not. The documents may come from teaching and research institutions in France or abroad, or from public or private research centers.

L'archive ouverte pluridisciplinaire **HAL**, est destinée au dépôt et à la diffusion de documents scientifiques de niveau recherche, publiés ou non, émanant des établissements d'enseignement et de recherche français ou étrangers, des laboratoires publics ou privés.

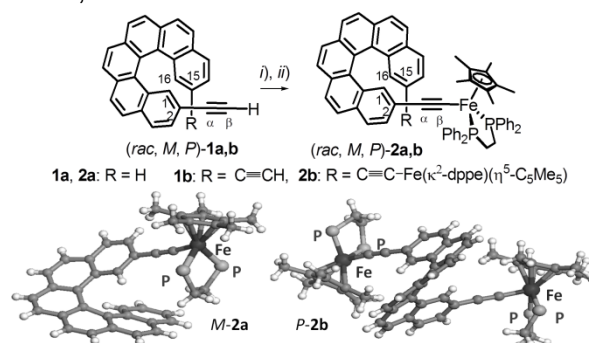
# Iron-alkynyl-helicenes: redox-triggered chiroptical tuning in the vibrational and telecommunication domain

Chengshuo Shen,<sup>[a]</sup> Goulc'hen Loas,<sup>[a]</sup> Monika Srebro-Hooper,<sup>[b]</sup> Nicolas Vanthuyne,<sup>[c]</sup> Loïc Toupet,<sup>[a]</sup> Olivier Cador,<sup>[a]</sup> Frédéric Paul,<sup>[a]</sup> Juan T. López Navarrete,<sup>[d]</sup> Francisco J. Ramírez,<sup>[d]</sup> Belén Nieto-Ortega,<sup>[d]</sup> Juan Casado,<sup>[d]</sup> Jochen Autschbach,<sup>\*,[e]</sup> Marc Vallet,<sup>[a]</sup> and Jeanne Crassous<sup>\*,[a]</sup>

**Abstract:** Combining In iron-alkynyl-iron moieties with a [6]helicene leads to novel electroactive species displaying unprecedented redox-triggered chiroptical switching. Upon oxidation, strong changes of vibrational modes, either local or extended coupled modes, are observed by vibrational circular dichroism and Raman optical activity. Remarkably, the optical rotation at 1.54 microns (telecommunication region) alters sign upon oxidation while the topology and stereochemistry of the helicene remain unchanged.

Molecular engineering combining helicene and organometallic chemistry has recently given access to multi-functional chiral systems displaying strong chiroptical properties and other functions furnished by the metal.<sup>[1,2]</sup> This new strategy is of great interest for many optoelectronic applications.<sup>[3]</sup> An interesting class of organometallic complexes are aryl-alkynyl-iron systems which display facile electron transfer<sup>[4]</sup> enabling the redox-triggering of their optical properties (NLO-activity,<sup>[4e,5a-c]</sup> luminescence,<sup>[5d,e]</sup> absorption and colour<sup>[5f]</sup>). In this communication, we describe unprecedented helicene-ethynyl mono- and bis-Fe(II) complexes **2a** and **2b** grafted respectively with one or two electroactive  $[\text{Fe}(\kappa^2\text{-dppe})(\eta^5\text{-C}_5\text{Me}_5)]$  fragments **3**<sup>[6]</sup> (Scheme 1) and their use as efficient redox-triggered chiroptical molecular switches.<sup>[7]</sup> We demonstrate for the first time how the chiroptical properties in the vibrational and telecommunication domains, by means of vibrational circular dichroism (VCD),<sup>[8]</sup> Resonance Raman Optical Activity (RROA),<sup>[9]</sup> as well as the molar rotation (MR) and electronic CD (ECD) at 1.54 microns, are influenced upon oxidation to radical cationic species.

The helicene-based mono- and bis-Fe(II) complexes (*rac,M,P*)-**2a,b** were prepared as air-stable red solids in good yields (51-77%) from alkynyl-[6]helicene ligands (*rac,M,P*)-**1a,b**,<sup>[2e,g]</sup> and **3-Cl**<sup>[6a]</sup> (Scheme 1). The synthesis proceeds *via* the formation of cationic iron-vinylidene intermediates followed



**Scheme 1.** Preparation of mono- and bis-iron-ethynyl-[6]helicene complexes **2a,b** from mono- and bis-ethynyl-[6]helicenes **1a,b**. *i*)  $\text{Fe}(\kappa^2\text{-dppe})(\eta^5\text{-C}_5\text{Me}_5)\text{Cl}$  (**3-Cl**), MeOH, THF,  $\text{NaPF}_6$ ; *ii*) THF,  $^t\text{BuOK}$ . X-ray crystal structures of enantiopure **M-2a** and racemic **2b** (*P* enantiomer shown). dppe Ph groups omitted for clarity.

by their deprotonation to the neutral complexes **2a,b**.<sup>[6]</sup> The Supporting Information (SI) provides a full characterization.

**M-2a** and ( $\pm$ )-**2b** crystallized in the  $P2_1$  and  $P-1$  space group, respectively. Their X-ray structures (Scheme 1, SI) show regular metric data for the piano-stool iron part (classical lengths for the  $\text{Fe-C}_\beta$ ,  $\text{C}_\alpha\text{-C}_\beta$  and  $\text{C}_\alpha\text{-C}_2$  bonds ca. 1.89, 1.22-1.23 and 1.42-1.43 Å),<sup>[6]</sup> and classical helical angles for [6]helicenic ligands (53.1-60.5°).<sup>[2]</sup> The linearity of the ethynyl fragments ensures an efficient  $\pi$ -conjugation between the helicene and the iron (angles  $\text{Fe-C}_\beta\text{-C}_\alpha$  of 173.7° and  $\text{C}_\beta\text{-C}_\alpha\text{-C}_2$  of 175.0°).

The chiroptical properties upon grafting one or two electroactive Fe (by way of fragment **3**) to a helicene-alkynyl moiety are strongly modified. For instance, the ECD spectrum of **P-2b** shows typical helicene bands *i.e.* an intense negative band at 300 ( $\Delta\epsilon = -125 \text{ M}^{-1} \text{ cm}^{-1}$ ) and strong positive bands at 337 ( $\Delta\epsilon = +110 \text{ M}^{-1} \text{ cm}^{-1}$ ) and 386 nm ( $\Delta\epsilon = +78 \text{ M}^{-1} \text{ cm}^{-1}$ , Figure 1). An additional intense broad positive band at 506 nm ( $\Delta\epsilon = +68 \text{ M}^{-1} \text{ cm}^{-1}$ ) corresponds to the HOMO→LUMO transition and affords charge transfer from fragment **3** to the helicene, as assigned by time-dependent density functional theory (TDDFT,<sup>[10]</sup> Figure 2 and SI). The HOMO of **2b** mainly extends over **3**, while the LUMO is mainly a helicene  $\pi^*$  orbital.

Cyclic voltammetry shows one reversible oxidation wave at -0.144 V (vs. SCE) for **2a** and two waves at -0.180 V and -0.089V for **2b** (SI). The one- (**2a**) and two-electron (**2b**) oxidation processes were monitored by ECD<sup>[2c,e]</sup> either chemically with iodine or spectroelectrochemically ( $\text{C}_2\text{H}_4\text{Cl}_2/\text{NBu}_4\text{PF}_6$ , 0.2 M). For example, upon oxidation of **P-2b** to **P-[2b]]<sup>•+</sup>** there is (*i*) a strong increase of the positive ECD band around 350 nm ( $\Delta(\Delta\epsilon) > +100 \text{ M}^{-1} \text{ cm}^{-1}$  at 372 nm), (*ii*) a strong decrease of the positive band between 530-650 nm with appearance of a negative band, and (*iii*) appearance of a broad band in the Vis-NIR (670-900 nm,  $\Delta(\Delta\epsilon) \sim +20 \text{ M}^{-1} \text{ cm}^{-1}$  at 767 nm); see Figure 1. Interestingly, an ECD band of the **M-[2b]]<sup>•+</sup>** oxidized species was also observed

[a] Dr. C. Shen, Dr. G. Loas, Dr. L. Toupet, Dr. O. Cador, Dr. F. Paul, Prof. M. Vallet, Dr. J. Crassous, Institut des Sciences Chimiques de Rennes UMR 6226, Institut de Physique de Rennes, UMR 6251, CNRS Université de Rennes 1, Campus de Beaulieu, 35042 Rennes Cedex (France). E-mail: jeanne.crassous@univ-rennes1.fr

[b] Dr. M. Srebro-Hooper, Faculty of Chemistry, Jagiellonian University, R. Ingardena 3, 30-060 Krakow (Poland)

[c] Dr. N. Vanthuyne, Aix Marseille Université, Centrale Marseille, CNRS, iSm2 UMR 7313, 13397, Marseille (France)

[d] Dr. Belén Nieto-Ortega, Prof. F. J. Ramírez, Prof. T. López Navarrete, Prof. J. Casado, Department of Physical Chemistry, University of Malaga, Campus de Teatinos s/n, Malaga 29071, Spain.

[e] Prof. J. Autschbach, Department of Chemistry, University at Buffalo, State University of New York, Buffalo, NY 14260 (USA). Email: jochena@buffalo.edu

Supporting information for this article is given via a link at the end of the document. (Please delete this text if not appropriate)

in the NIR telecommunication domain, 1540 nm ( $\Delta\epsilon = -0.09 \text{ M}^{-1} \text{ cm}^{-1}$ ). All these ECD oxidation-induced changes are well reproduced by calculations (Figure 2; see SI for the MO analysis). Upon reduction, the spectral changes reversed and  $[2b]^{*2+}$  changed back to **2b**. The reversible redox modifications of the ECD spectra mean that **2a,b** behave as chiroptical switches (Figure 1c and SI).<sup>[2c,e,3b,7]</sup>

Relative to their organic precursors, **2a,b** display molar rotations (MRs) (*D*-line, 589 nm) that are strongly enhanced by the proximity to an electronic resonance (e.g. **P-2b** (**P-1b**)<sup>[2c,e]</sup>:  $[\Phi]_D^{23} = +79700^\circ (+20000^\circ) \text{ cm}^2/\text{dmol}$  (calc. 83844 (22230))). Upon oxidation, the MRs of **2a,b** undergo a strong (4 to 10-fold) decrease in magnitude. This can be rationalized by the corresponding changes in the ECD spectrum around 500 nm, which have a compensating effect on the optical rotation (e.g. **P-2b**  $\rightarrow$  **P-[2b]<sup>\*2+</sup>**, 2l:  $[\Phi]_D^{23} = +79700 \rightarrow +8990^\circ \text{ cm}^2/\text{dmol}$ , SI).

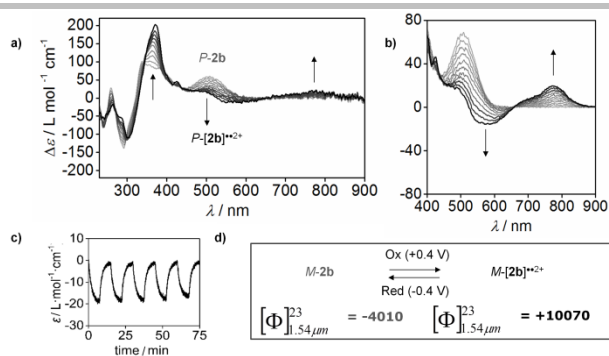


**Figure 1.** Oxidation of **P-2b** observed by ECD a) from the UV to the NIR region and b) in the 400-900 nm region. c) Redox chiroptical switching of **M-2b**  $\leftrightarrow$  **M-[2b]<sup>\*2+</sup>** observed by ECD at 767 nm (at  $\pm 0.4 \text{ V}$  vs. a Pt pseudo-potential reference electrode). d) Modification of the molar rotation values in the telecommunication domain (1.54  $\mu\text{m}$ ,  $\text{CH}_2\text{Cl}_2$ ,  $\text{C}$  10 mg/mL).

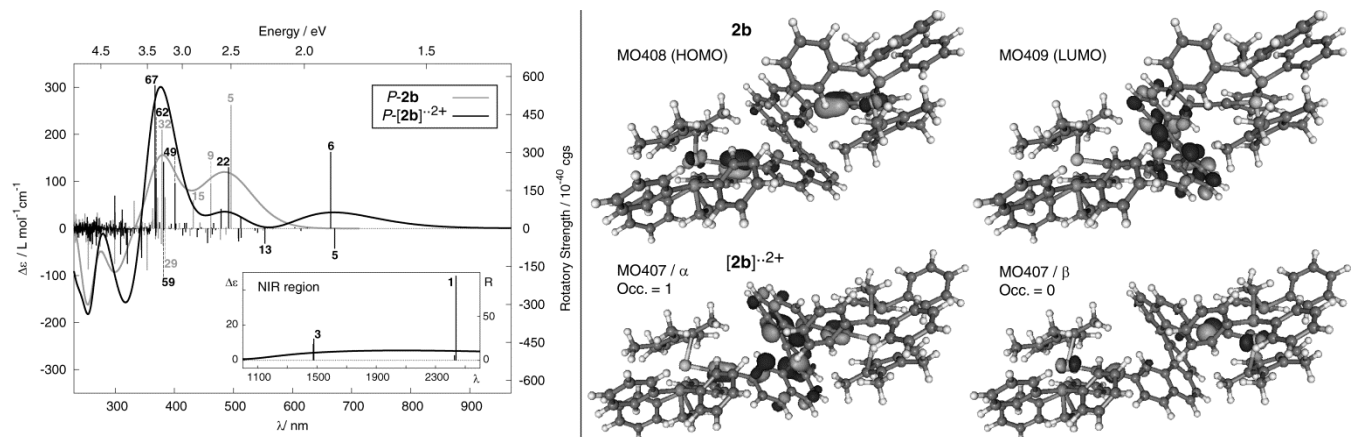


**Figure 2.** Left: Simulated B3LYP/SV(P) ECD spectra of **P-2b** (red) and **P-[2b]<sup>\*2+</sup>** (black). Calculated excitation energies and rotatory strengths indicated as 'stick' spectra. Numbered excitations were analyzed in detail (SI). Inset: NIR ECD of **P-2b** and **P-[2b]<sup>\*2+</sup>**. Right: Isosurfaces (0.04 au) of frontier MOs of **2b** / **[2b]<sup>\*2+</sup>**.

Stimulus-responsive materials in the telecommunication domain may be of great interest for transmitting encoded information.<sup>[11]</sup> Interestingly, using an in-house developed polarimeter, molar rotations of  $-2370$  and  $-4010^\circ \text{ cm}^2/\text{dmol}$  for **M-2a** and **M-2b**, respectively, were measured at 1.54  $\mu\text{m}$ , *i.e.* providing the transmitted light with a chiroptical tag, which *inverts its sign* upon oxidation processes **M-2a**  $\rightarrow$  **M-[2a]<sup>\*+</sup>** (SI) and **M-2b**  $\rightarrow$  **M-[2b]<sup>\*2+</sup>** (Figure 1d). These drastic changes illustrate well the potential of efficiently tuning or even reversing chiroptical properties at telecommunication wavelengths while keeping the integrity of the helical backbone. They can be rationalized by the presence of ECD-active electronic excitations around 1.54  $\mu\text{m}$  for the oxidized species, which results in anomalous OR dispersion that can change the sign of the OR.<sup>[10b,12]</sup> This case therefore constitutes a new type of redox-triggered chiroptical switch using a clear output tag at 1.54  $\mu\text{m}$  *i.e.* outside the more common wavelength regions.

Apart from electronic ECD and optical rotation, vibrational optical activity, *i.e.* VCD and ROA,<sup>[12]</sup> provide additional molecular level information related to the chirality and redox switching. Figure 3 shows the IR and VCD spectra of enantiopure complexes **M-** and **P-2b** and **M-** and **P-[2b]<sup>\*2+</sup>**. Several interesting spectroscopic features are found. In particular, (i) a strong IR and VCD-active mode at  $2046 \text{ cm}^{-1}$  corresponding to the  $\text{C}\equiv\text{C}$  stretch, with positive VCD sign, (ii) two

negative-positive signatures at 1595-1566 and  $1500\text{-}1485 \text{ cm}^{-1}$  belonging to  $\text{C}=\text{C}$  stretches coupled with CCH bending (SI).<sup>[2d]</sup> Upon chemical oxidation with iodine, the  $\text{C}\equiv\text{C}$  stretching band appears split and at lower wavenumbers ( $1996$  and  $2032 \text{ cm}^{-1}$ ), probably due to Fermi coupling,<sup>[6b]</sup> with a negative-positive VCD pattern. The wavenumber decrease is probably due to delocalization of the hole into the acetylene spacer which thus acquires some cumulenic  $\text{C}=\text{C}=\text{Fe}$  character. More interestingly, a 30-fold increase of the dissymmetry factor is observed upon oxidation ( $g = \Delta\epsilon/\epsilon$  from  $3.10^{-4}$  to  $10^{-2}$ ). The strong enhancement supports the presence of electron spin density within the  $\text{C}\equiv\text{C}$  moiety which may give rise to stronger magnetic transition dipole moments within the vibrational transitions. Indeed, the paramagnetic character of radical cationic species **P-[2a]<sup>\*+</sup>** and **P-[2b]<sup>\*2+</sup>** are clearly evidenced by susceptibility and  $^1\text{H}$  NMR measurements (SI) and calculations show how spin density delocalizes from the metal into the helical backbone (Figure S40). Low-lying electronic states can also account for such enhancement.<sup>[13]</sup> To our knowledge this is the first time that such an increase is observed upon modifying the electron density of a helicenic species. Note that other modifications are observed in the  $1600\text{-}1450 \text{ cm}^{-1}$  region, and very similar trends were obtained for the monometallic complex **2a** (SI).

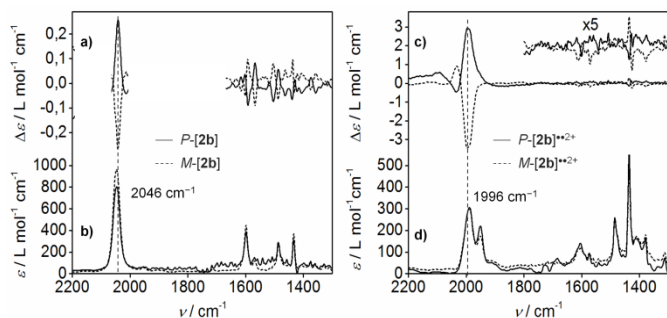


**Figure 3.** Experimental a) and c) VCD spectra of *M*- and *P*-**2b** and *M*- and *P*-**[2b]\*\*<sup>2+</sup>** b) and d) IR spectra of *M*- and *P*-**2b** and *M*- and *P*-**[2b]\*\*<sup>2+</sup>** (CD<sub>2</sub>Cl<sub>2</sub>, *C* ~ 3 · 10<sup>-3</sup> M).

To date, (Resonance) Raman and ROA spectroscopy,<sup>[12]</sup> which are complementary techniques to IR and VCD, are far less utilized in helicene chemistry and in coordination chemistry.<sup>[9]</sup> For **2a,b** (Figure 4, SI), three modes were found to be strongly Raman active: the G-mode (graphene-like CC stretching mode) at 1594 cm<sup>-1</sup>, the D-mode (diamond-like CC breathing mode) at 1355 cm<sup>-1</sup> and the C≡C stretching mode at 2046 cm<sup>-1</sup>.<sup>[9a,14]</sup> Noteworthy, all ROA bands display the same sign, *i.e.* negative for the *P* enantiomers and all positive for the *M* ones. The experimental wavelength used for measurements (532 nm) coincides with an electronic absorption band of the spectra for both **2a** and **2b**, which implies that what we observe is resonant ROA (RROA).<sup>[12,15]</sup> The RROA signals are: *i*) monosignate; *ii*) of reverse sign as the ECD band at the 532 nm resonant Raman excitation; and *iii*) the dissymmetry factors *g* of the ECD regarding those of the RROA overall follow a *g*(RROA) = - *g*(ECD)/2 relationship. For instance, in *P*-**[2b]\*\*<sup>2+</sup>** the RROA bands have *g* = -0.002 while the corresponding value for the ECD is *g* = +0.004. These features are in agreement with the ROA expected for a single electronic state resonance situation.<sup>[15]</sup> Here again, iodine oxidation provokes significant modifications of the Raman and ROA spectra, and complementarily to VCD shows that not only the C≡C stretching mode is affected (changing from 2046 to 1988 cm<sup>-1</sup>) but also the G- and D-modes (Figure 4, SI) confirming the involvement and alteration of the π-conjugated structure within the helicene core. To our knowledge, this is the first time where ROA is used for examining modifications upon redox changes. This technique may be useful for studying other chiral systems such as chiral fullerenes or carbon nanotubes.<sup>[14]</sup>

In summary, we have shown that while keeping the integrity of their structure, organometallic helicenes can invert their optical rotation at 1.54 microns upon oxidation. Furthermore, VCD and ROA spectroscopy provide molecular level description of the effect of redox neutral→cation switch at the origin of the several 10-fold magnitude increase along with frequency shifts. The switching described in the present article demonstrates the possibility to select the dichroic signal of an incoming circularly polarized light beam in the vibrational and telecommunication domain. Presently, light encoding processes for optical information treatments are achieved by ultrafast optical switching. Future research will need to focus on improving the speed of the switching processes in solid-state device prototypes.

## Acknowledgements

This work was supported by the ANR (12-BS07-0004-METALHEL-01), the French Ministry of Research, and the CNRS (project DIL "CARIM"). MS-H acknowledges the FNP Homing Plus programme cofinanced by EU funds and a Ministry of Science and Higher Education in Poland scholarship. JA acknowledges NSF Grant CHE-1265833 and the Center for Computational Research in Buffalo for computational support.

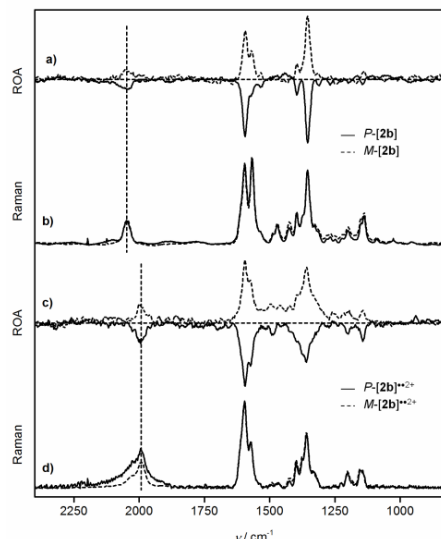


**Figure 4.** Experimental a) and c) ROA spectra of *M*- and *P*-**2b** and *M*- and *P*-**[2b]\*\*<sup>2+</sup>** b) and d) Raman spectra of *M*- and *P*-**2b** and *M*- and *P*-**[2b]\*\*<sup>2+</sup>** (CH<sub>2</sub>Cl<sub>2</sub>, *C* ~ 3 · 10<sup>-3</sup> M).

**Keywords:** organometallic helicenes, ROA, VCD, optical rotation, telecommunication

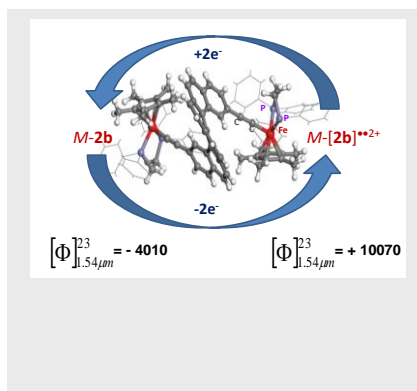
- [1] Selected reviews on helicenes properties: a) Y. Shen, C. -F. Chen, *Chem. Rev.* **2012**, 112, 1463; b) M. Gingras, *Chem. Soc. Rev.* **2013**, 42, 1051; c) N. Saleh, C. Shen, J. Crassous, *Chem. Sci.* **2014**, 5, 3680.
- [2] a) L. Norel, M. Rudolph, N. Vanthuyne, J. A. G. Williams, C. Lescop, C. Roussel, J. Autschbach, J. Crassous, R. Réau, *Angew. Chem. Int. Ed.* **2010**, 49, 99; b) E. Anger, M. Rudolph, C. Shen, N. Vanthuyne, L. Toupet, C. Roussel, J. Autschbach, J. Crassous, R. Réau, *J. Am. Chem. Soc.* **2011**, 133, 3800; c) E. Anger, M. Srebro, N. Vanthuyne, L. Toupet, S. Rigaut, C. Roussel, J. Autschbach, J. Crassous, R. Réau, *J. Am. Chem. Soc.* **2012**, 134, 15628; d) E. Anger, M. Srebro, N. Vanthuyne, C. Roussel, L. Toupet, J. Autschbach, R. Réau, J. Crassous, *Chem. Comm.* **2014**, 50, 2854; e) M. Srebro, E. Anger, B. Moore, II, N. Vanthuyne, C. Roussel, R. Réau, J. Autschbach, J. Crassous, *Chem. Eur. J.* **2015**, 21, 17100.
- [3] a) Y. Yang, R. C. da Costa, M. J. Fuchter, A. J. Campbell, *Nature Photonics* **2013**, 7, 634; b) D. Schweinfurth, M. Zalibera, M. Kathan, C. Shen, M. Mazzolini, N. Trapp, J. Crassous, G. Gescheidt, F. Diederich, *J. Am. Chem. Soc.* **2014**, 136, 13045; c) R. A. van Delden, M. K. J. ter Wiel, M. M. Pollard, J. Vicario, N. Koumura, B. L. Feringa, *Nature* **2005**, 437, 1337; d) T. R. Kelly, H. De Silva, R. A. Silva, *Nature* **1999**, 401, 150; e) T. Verbiest, S. Van Elshocht, M. Kauranen, L. Hellemans, J. Snauwaert, C. Nuckolls, T. J. Katz, A. Persoons, *Science* **1998**, 282, 913; f) L. Pospisil, L. Bednarova, P. Stepánek, P. Slavicek, J. Vavra, M. Hromádova, H. Dlouha, J. Tarabek, F. Těplý, *J. Am. Chem. Soc.* **2014**, 136, 10826.
- [4] a) F. Paul, C. Lapinte, *Coord. Chem. Rev.* **1998**, 178, 431; b) P. Aguirre-Etcheverry, D. O'Hare, *Chem. Rev.* **2010**, 110, 4839; c) G. Grelaud, M. P. Cifuentes, F. Paul, M. G. Humphrey, *J. Organomet. Chem.* **2014**, 751, 181; d) J. -F. Halet, C. Lapinte, *Coord. Chem. Rev.* **2013**, 257, 1584; e) B. J. Coe, *Coord. Chem. Rev.* **2013**, 257, 1438.

- [5] a) M. Samoc, N. Gauthier, M. P. Cifuentes, F. Paul, C. Lapinte, M. G. Humphrey, *Angew. Chem. Int. Ed.* **2006**, *45*, 7376; b) C. E. Powell, M. P. Cifuentes, J. P. Morrall, R. Stranger, M. G. Humphrey, M. Samoc, B. Luther-Davies, G. A. Heath, *J. Am. Chem. Soc.* **2003**, *125*, 602; c) K. A. Green, M. P. Cifuentes, T. C. Corkery, M. Samoc, M. G. Humphrey, *Angew. Chem. Int. Ed.* **2009**, *48*, 7867; d) E. Di Piazza, L. Norel, K. Costuas, A. Bourdolle, O. Maury, S. Rigaut, *J. Am. Chem. Soc.* **2011**, *133*, 6174; e) M. Murai, M. Sugimoto, M. Akita, *Dalton Trans.* **2013**, *42*, 16108; f) Y. Tanaka, T. Ishisaka, A. Inagaki, T. Koike, C. Lapinte, M. Akita, *Chem. Eur. J.* **2010**, *16*, 4762.
- [6] a) C. Roger, P. Hamon, L. Toupet, H. Rabaa, J.-Y. Saillard, J. -R. Hamon, C. Lapinte, *Organometallics* **1991**, *10*, 1045; b) F. Paul, J. -Y. Mevellec, C. Lapinte, *Dalton Trans.* **2002**, 1783; c) F. Paul, A. Bondon, G. da Costa, F. Malvotti, S. Sinbandhit, O. Cadot, K. Costuas, L. Toupet, M. -L. Boillot, *Inorg. Chem.* **2009**, *48*, 10608; d) K. Costuas, F. Paul, L. Toupet, J.-F. Halet, C. Lapinte, *Organometallics* **2004**, *23*, 2053.
- [7] See H. Isla, J. Crassous, *Comptes Rendus Chimie*, **2016**, doi: 10.1016/j.crci.2015.06.014 and references therein.
- [8] a) T. Bürgi, A. Urakawa, B. Behzadi, K.-H. Ernst, A. Baiker, *New. J. Chem.* **2004**, *28*, 332; b) S. Abbate, F. Lebon, G. Longhi, F. Fontana, T. Caronna, D. A. Lightner, *Phys. Chem. Chem. Phys.* **2009**, *11*, 9039; c) S. Abbate, G. Longhi, F. Lebon, E. Castiglioni, S. Superchi, L. Pisani, F. Fontana, F. Torricelli, T. Caronna, C. Villani, R. Sabia, M. Tommasini, A. Lucotti, D. Mendola, A. Mele, D. A. Lightner, *J. Phys. Chem. C* **2014**, *118*, 1682; d) T. B. Freedman, X. Cao, A. Rajca, H. Wang, L. A. Nafie, *J. Phys. Chem. A* **2003**, *107*, 7692; e) F. Torricelli, J. Bosson, C. Besnard, M. Chekini, T. Bürgi, J. Lacour, *Angew. Chem. Int. Ed.* **2013**, *52*, 1796; f) V. P. Nicu, J. Neugebauer, S. K. Wolff, E. J. Baerends, *Theor. Chem. Account* **2008**, *119*, 245; g) V. Liégeois, B. Champagne, *J. Comput. Chem.* **2009**, *30*, 1261.
- [9] Experimental ROA of helices: a) C. Johannessen, E. W. Blanch, C. Villani, S. Abbate, G. Longhi, N. R. Agarwal, M. Tommasini, D. A. Lightner, *J. Phys. Chem. B* **2013**, *117*, 2221; theoretical ROA of helices: b) V. Liégeois, B. Champagne, *Theor. Chem. Acc.* **2012**, *131*, 1284; c) M. Tommasini, G. Longhi, G. Mazzeo, S. Abbate, B. Nieto-Ortega, F. J. Ramírez, J. Casado, J. T. L. Navarrete, *J. Chem. Theory Comput.* **2014**, *10*, 5520; d) S. Yamamoto, P. Bour, *Angew. Chem. Int. Ed.* **2012**, *51*, 11058.
- [10] a) J. Autschbach, *Chirality* **2009**, *21*, E116; b) J. Autschbach, L. Nitsch-Velasquez, M. Rudolph, *Top. Curr. Chem.* **2011**, *298*, 1.
- [11] G. P. Agrawal, *Fiber-optic Communication Systems*, 4th Ed., Wiley, **2010**.
- [12] a) L. D. Barron, *Molecular Light Scattering and Optical Activity*, 2nd Edition, Cambridge, **2009**; b) L. A. Nafie, *Vibrational Optical Activity: Principles and Applications*, Wiley, **2011**.
- [13] a) Y. He, X. Cao, L. A. Nafie, T. B. Freedman, *J. Am. Chem. Soc.* **2001**, *123*, 11320; b) S. R. Domingos, A. Huerta-Viga, L. Baij, S. Amirjalayer, D. A. E. Dunnebie, A. J. C. Walters, M. Finger, L. A. Nafie, B. de Bruin, W. J. Buma, S. Woutersen, *J. Am. Chem. Soc.* **2014**, *136*, 3530 and references therein.
- [14] a) E. Di Donato, M. Tommasini, G. Fustella, L. Brambilla, C. Castiglioni, G. Zerbi, C. D. Simpson, K. Mullen, F. Negri, *Chem. Phys.* **2004**, *301*, 81; b) C. Castiglioni, M. Tommasini, G. Zerbi, *Philos. Trans. R. Soc., A* **2004**, *362*, 2425; c) M. Tommasini, C. Castiglioni, G. Zerbi, *Phys. Chem. Chem. Phys.* **2009**, *11*, 10185; d) A. C. Grimsdale, K. Mullen, *Angew. Chem. Int. Ed.* **2005**, *44*, 5592.
- [15] a) L. A. Nafie, *Chem. Phys.* **1996**, *205*, 309; b) M. Vargak, T. B. Freedman, E. Lee, L. A. Nafie, *Chem. Phys. Lett.* **1998**, *287*, 359; c) L. Jensen, J. Autschbach, M. Krykunov, G. C. Schatz, *J. Chem. Phys.* **2007**, *127*, 134101.



## COMMUNICATION

[6]Helicene-alkynyl-iron complexes have been prepared and used to finely examine, by VCD and ROA spectra, how the oxidation to radical cations influences their vibrational modes. Moreover, these chiral organometallic species display a sign change of their optical rotation in the telecommunication domain (1.54 microns), while their molecular structures keep their integrity.



C. Shen, G. Loas, M. Srebro-Hooper, N. Vanthuyne, L. Toupet, O. Cador, F. Paul, J. T. López Navarrete, F. J. Ramírez, B. Nieto-Ortega, J. Casado, J. Autschbach,\* M. Vallet, and J. Crassous\*

*Author(s), Corresponding Author(s)\**

**Page No. – Page No.**

**Iron-alkynyl-helicenes: redox-triggered chiroptical tuning in the vibrational and telecommunication domain**

